Eur Biophys J (2006) 35: 495–501
DOI 10.1007/s00249-006-0057-7

ARTICLE

Silvia Caño · Juan Manuel Caravaca
Marc Martín · Joan-Ramon Daban

Highly compact folding of chromatin induced by cellular cation concentrations. Evidence from atomic force microscopy studies in aqueous solution

Received: 21 December 2005 / Revised: 10 March 2006 / Accepted: 14 March 2006 / Published online: 30 March 2006
© EBSA 2006

Abstract We have performed a very extensive investigation of chromatin folding in different buffers over a wide range of ionic conditions similar to those found in eukaryotic cells. Our results show that in the presence of physiological concentrations of monovalent cations and/or low concentrations of divalent cations, small chicken erythrocyte chromatin fragments and chromatin from HeLa cells observed by transmission electron microscopy (TEM) show a compact folding, forming circular bodies of approximately 35 nm in diameter that were found previously in our laboratory in studies performed under very limited conditions. Since TEM images are obtained with dehydrated samples, we have performed atomic force microscopy (AFM) experiments to analyze chromatin structure in the presence of solutions containing different cation concentrations. The highly compact circular structures (in which individual nucleosomes are not visible as separated units) produced by small chromatin fragments in interphase ionic conditions observed by AFM are equivalent to the structures observed by TEM with chromatin samples prepared under the same ionic conditions. We have also carried out experiments of sedimentation and trypsin digestion of chromatin fragments; the results obtained confirm our AFM observations. Our results suggest that the compaction of bulk interphase chromatin in solution at room temperature is considerably higher than that generally considered in current literature. The dense chromatin folding observed in this study is consistent with the requirement of compact chromatin structures as starting elements for the building of metaphase chromosomes, but poses a difficult physical problem for gene expression during interphase.

S. Caño · J. M. Caravaca · M. Martín · J.-R. Daban (✉)
Departament de Bioquímica i Biologia Molecular,
Facultat de Ciències, Universitat Autònoma de Barcelona,
08193 Bellaterra, Barcelona, Spain
E-mail: joanramon.daban@uab.es
Fax: +34-93-5811264

Keywords Chromatin structure · Atomic force microscopy · Transmission electron microscopy · Intracellular cation concentrations

Abbreviations AFM: Atomic force microscopy · CE: Chicken erythrocyte · TEA: Triethanolamine–HCl buffer (pH 7.5) · TEM: Transmission electron microscopy

Introduction

The linear packing ratio of DNA in condensed chromatin within metaphase chromosomes is high (Sumner 2003). At present, we know from X-ray crystallographic studies the detailed three-dimensional structure of the DNA coiled around the histone octamer in the nucleosome (Arents et al. 1991; Luger et al. 1997; Harp et al. 2000; White et al. 2001; Richmond and Davey 2003). This fundamental chromatin subunit, completed with linker DNA and one molecule of histone H1 (or H5 in avian erythrocytes), forms fibers of 30–40 nm in diameter (Widom 1998; Hansen 2002; Zlatanova and Leuba 2003). Different structural models have been suggested for these fibers (Widom and Klug 1985; Subirana et al. 1985; Bordas et al. 1986; Williams et al. 1986; Leuba et al. 1994; Bednar et al. 1998; Daban and Bermúdez 1998; Mozziconacci and Victor 2003; Grigoryev 2004; Schalch et al. 2005), but we have a poor knowledge of the higher levels of folding that produce the chromatin condensation observed during mitosis (Wolffe 1998; Woodcock and Dimitrov 2001; Marko and Poirier 2003). We have pointed out (Daban 2000, 2003) that the high local DNA concentration (0.17 g/ml) found in metaphase chromosomes constitutes a physical constraint that must be considered in the construction of structural models for condensed chromatin.

Chromatin folding is dependent on the concentration of mono- and divalent cations (Widom 1986, 1998;

Hansen 2002; Poirier et al. 2002). Thus, for the understanding of chromatin structure in the cell we must know the actual in vivo ionic conditions. We know that in eukaryotic cells the concentrations of the monovalent cations Na^+ and K^+ are approximately 20 and 120 mM, respectively (Alberts et al. 2002), but the available experimental data for other cations have been very limited. This situation has changed thanks to the ion microscopy study of Strick et al. (2001) which has allowed the determination of the three-dimensional distribution of the cations present in interphase and mitotic cells. These authors have used a high-resolution scanning ion microprobe (Levi-Setti 1988) for imaging and microanalysis of cryopreserved cells and fixed metaphase chromosomes by secondary ion mass spectrometry. They have found that only the cations Na^+, K^+, Mg^{2+}, and Ca^{2+} are associated with metaphase chromosomes, and that whereas the distribution of Na^+ and K^+ remains unchanged during the cell cycle, the Mg^{2+} and Ca^{2+} concentrations found in mitotic chromatin (5–17 and 12–24 mM, respectively) are higher than those found in interphase nuclei (2–4 and 4–6 mM, respectively). Furthermore, their results indicate that Na^+, K^+, and Mg^{2+} are distributed homogeneously over the entire metaphase chromosome, but Ca^{2+} is mainly located in the chromatid axes, presumably associated with topoisomerase II.

The huge molecular mass and intrinsic irregularity of the higher order structures of chromatin have made very difficult the study of this complex supramolecular system. In order to overcome, at least in part, these difficulties we developed in previous studies a simple experimental system to investigate chromatin structure by transmission electron microscopy (TEM). These studies (Bartolomé et al. 1994, 1995) were carried out using small native chromatin fragments (containing the native amount of linker histones H5/H1) obtained from chicken erythrocytes (CE). In this work we have used this system for a very extensive investigation of chromatin structure in different buffers over a wide range of ionic conditions. We have also extended our investigation to chromatin from cells containing exclusively the typical linker histone H1 instead of the very basic linker histone variant H5 of CE; we have studied chromatin from nuclei and metaphase chromosomes of HeLa cells. Since TEM has been criticized because it requires specimen dehydration (Leuba et al. 1994; Woodcock and Horowitz 1997), we have used atomic force microscopy (AFM) to analyze the structure of chromatin at room temperature in the presence of aqueous solutions containing different ionic compositions. Furthermore, we have also carried out sedimentation and trypsin digestion experiments of chromatin fragments in solution to corroborate our AFM observations. Our results show that extended chromatin fibers, with nucleosomes present as separated units, exist in solution only at very low ionic strength. Chromatin becomes densely packed even in the presence of the low Mg^{2+} concentration found in interphase.

Materials and methods

Chromatin fragments from chicken erythrocytes

CE nuclei were prepared by sedimentation on a discontinuous sucrose gradient (Rill et al. 1978) and digested with micrococcal nuclease as described elsewhere (Bartolomé et al. 1994). Soluble chromatin was extracted overnight at 4°C with 10 mM TEA, 40 mM NaCl, 1 mM EDTA, and 0.4 mM PMSF, concentrated (with Centriprep-10, Amicon) to 8–16 mg/ml of DNA, and fractionated by a 5–20% sucrose gradient containing 10 mM TEA, 5 mM EDTA, and 0.4 mM PMSF. Selected chromatin fractions were diluted or dialyzed to adjust the final ionic conditions indicated in the figure legends. In some experiments the selected fractions were further electrophoresed on 0.5% agarose gels in the presence of 90 mM Tris–borate (pH 8.3) and 1.7 mM $MgCl_2$ (Bartolomé et al. 1995). The isolated DNA from the different samples was analyzed on agarose gels; the mean number of nucleosomes of the chromatin fragments was estimated considering that the length of DNA of a single nucleosome is approximately 210 bp for chicken erythrocytes (Williams and Langmore 1991). Unless otherwise indicated the fragments used in this study contained ~20 nucleosomes. The histone composition of the different samples was analyzed on SDS-polyacrylamide gels.

Chromatin fragments and metaphase chromosomes from HeLa cells

HeLa cells were grown in DMEM medium (Gibco) supplemented with 10% fetal bovine serum. Nuclei were obtained in 10 mM TEA, 30 mM NaCl, 90 mM KCl, 0.15 mM spermine, 0.5 mM spermidine, and 0.4 mM PMSF, digested with micrococcal nuclease, and extracted overnight as described above for CE nuclei. The resulting soluble chromatin was concentrated (with Centricon-10, Amicon) to approximately 0.5 mg/ml of DNA and fractionated directly by electrophoresis on 0.5% agarose gels in the presence of 1.7 mM $MgCl_2$ (Bartolomé et al. 1995). After electrophoresis, the selected bands were excised from the gel and used for electron microscopy experiments. Cultures were treated with 0.1 μg/ml of colcemid (Gibco) for 14 h prior to the isolation of mitotic cells by shaking. Generally, unfixed metaphase chromosomes were isolated and purified on sucrose gradients containing 5 mM Pipes (pH 7.2), 5 mM NaCl, 5 mM $MgCl_2$, and 1 mM EGTA as described elsewhere (Caravaca et al. 2005). In some experiments chromosomes were prepared following diverse modifications of this procedure; in particular, in the sample shown in Fig. 1d, the buffer used in the initial steps contained 1 mM $CaCl_2$ and 5 mM $MgCl_2$ instead of 0.2 mM spermine and 0.5 mM spermidine used in the original procedure.

TEM

Prior to spreading on carbon-coated copper grids, chromatin fragments were crosslinked with 0.1% glutaraldehyde for 16 h at 4°C. Chromosome spreading was performed by centrifugation (Caravaca et al. 2005); the grids were floated face down in 0.3–0.5 ml-drops containing the solution indicated in the legend of Fig. 1, and incubated at 37°C for 30 min. Chromosomes were fixed on the grids with 2.5% glutaraldehyde for 10 min at 20°C. Specimens were dehydrated in ethanol and rotary-shadowed with platinum (Aragay et al. 1991).

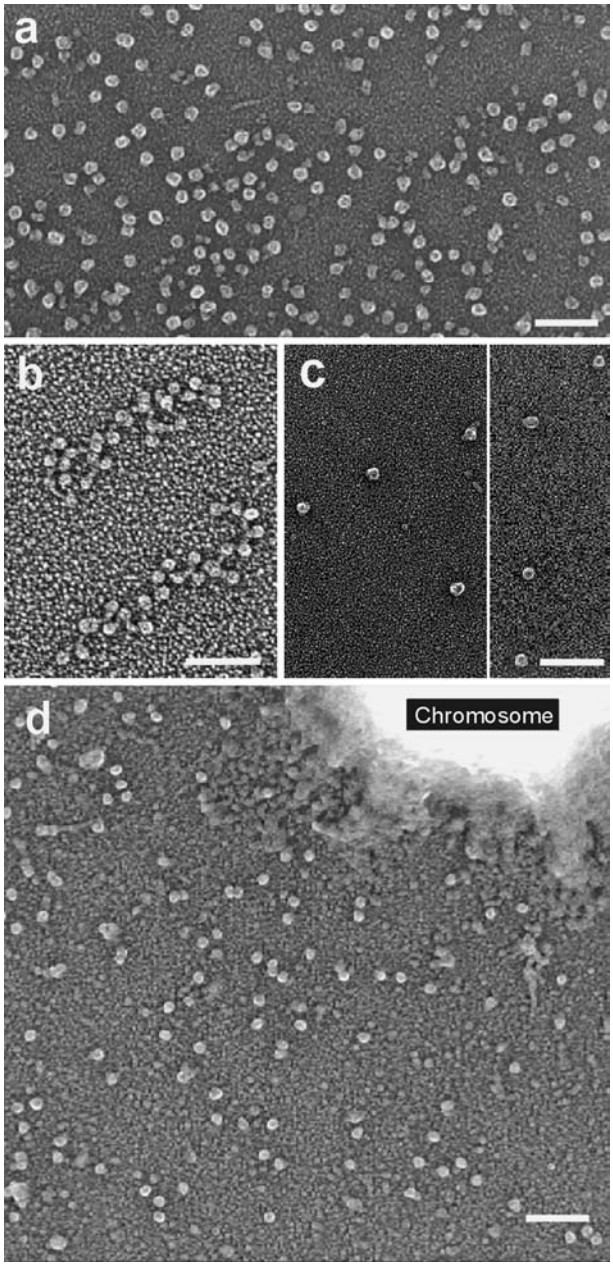

Fig. 1 Examples of chromatin folding as seen by TEM. CE chromatin fragments in 10 mM phosphate, 20 mM NaCl, 120 mM KCl and 1.7 mM $MgCl_2$ (**a**) and in diluted buffer (0.5 mM TEA) without cations (**b**). **c** Chromatin fragments from HeLa cells in 90 mM triethanolamine-borate and 1.7 mM $MgCl_2$. **d** Chromatin granules dispersed around a HeLa metaphase chromosome incubated in 50 mM TEA, 25 mM KCl, 1 mM $CaCl_2$ and 1.7 mM $MgCl_2$; only part of a chromatid is shown. *Bars*: 200 nm (**a**, **c**, **d**); 100 nm (**b**)

AFM

Imaging was performed with a Nanoscope-IV Multimode microscope (Digital Instruments) equipped with a tapping-mode liquid cell and a silicon nitride OMCL-TR400PSA-1 tip (~20 nm radius) mounted on a 100-μm triangular cantilever (Olympus). Chromatin samples were adsorbed on freshly cleaved mica or highly oriented pyrolytic graphite for 5 min and washed with the buffer corresponding to each experiment. Images were obtained at room temperature.

Analysis of chromatin folding in sucrose gradients and trypsin digestions

Small volumes (0.23 ml) of a solution of CE chromatin fragments in 10 mM TEA were layered onto 5–20% sucrose gradients (4 ml) and centrifuged (100,000 g; 2 h at 4°C). Fractions were collected using a density gradient fractionator (AutoDensi-Flow, HaakeBuchler). Chromatin fragments were digested with trypsin at 20°C. Trypsin concentration and incubation time were varied widely to obtain samples with different digestion degrees. The partially digested histones of the resulting samples were dissolved in a buffer containing 2% SDS and analyzed in SDS-polyacrylamide gels.

Results and discussion

Nucleosomes can be seen in TEM micrographs as separated units in extended fibers prepared in 0.5 mM TEA (Fig. 1b). In solutions of higher ionic strength, chromatin fragments form compact circular structures with a diameter of ~35 nm (Fig. 1a) in which individual nucleosomes are apparently not visible at all. In previous studies of our laboratory (Bartolomé et al. 1994) we observed the formation of the same compact structures with chromatin fragments containing from 6 to 35 nucleosomes. In these studies, we demonstrated the formation of these structures only under limited conditions. In the present work we have found that different buffers (10 mM TEA, pH 7.5; 10 mM phosphate, pH 7.8; 90 mM triethanolamine-borate, pH 8.6) containing different amounts of mono- and divalent cations give rise to compact structures of ~35 nm; the approximate ionic conditions that produce these structures in TEA and phosphate buffers are indicated in Table 1. Our results show that compact chromatin exist in solutions containing low concentrations of Mg^{2+} (up to ~2 mM)

and/or physiological concentrations of Na^+ and K^+. At higher concentrations of Mg^{2+} (up to 20 mM), CE chromatin fragments produce aggregates of very high molecular mass.

Chromatin fragments obtained from cultures of HeLa cells, in the presence of 1.7 mM Mg^{2+}, also form the compact structures found with CE chromatin (Fig. 1c). Furthermore, in a recent study (Caravaca et al. 2005) we have observed that HeLa metaphase chromosomes incubated with solutions of low ionic strength become swelled and their chromatin forms granules of ~35 nm with the same structural characteristics as folded chromatin fragments. At higher ionic strength metaphase chromosomes are not granulated and have a compact structure. However, our results (Fig. 1d) show that circular structures of ~35 nm can also be seen in the chromatin extruded from compact chromosomes partially denatured after incubation at 37°C. These results suggest that chromatin has a high tendency to form these compact bodies. This could be related with early studies (Zentgraf and Franke 1984) showing the presence of superbeads in chromatin from different species.

All the above results have been obtained with dehydrated chromatin samples prepared according to current TEM protocols. In order to avoid specimen dehydration, other authors used cryo-electron microscopy to visualize frozen-hydrated preparations of chromatin (Bednar et al. 1998). These studies allowed high-resolution imaging of extended fibers at low ionic strength with nucleosomes clearly visible as separated units; even at intermediate concentrations of monovalent cations, in the absence of divalent cations, frozen-hydrated samples show resolved nucleosomes connected with extended linker DNA (Woodcock and Horowitz 1997). Other authors used AFM which, in the tapping-mode, allows imaging of chromatin samples in air and in aqueous solutions (Bustamante et al. 1997). To obtain high-resolution images of extended fibers, these studies were performed with air-dried samples prepared in the presence of low cation concentrations (Leuba et al. 1994). Ultra-high resolution imaging of DNA in nucleosomes has been recently obtained using AFM performed in ultra-high vacuum with dried samples (Davies et al. 2005). Unfortunately, AFM of chromatin in solution yields poorly resolved images and requires glutaraldehyde (0.1%) to improve the resolution (Leuba et al. 2000).

In this study, we have performed tapping-mode AFM imaging of small CE chromatin fragments directly in aqueous solutions at room temperature. Chromatin in different ionic conditions was deposited on mica (Fig. 2a, c) or graphite (Fig. 2b, d). We have found that crosslinking with low amounts of glutaraldehyde (0.01–0.02% in mica and 0.04% in graphite) is adequate for chromatin imaging in solution. In Na^+, K^+ and Mg^{2+} concentrations approaching the interphase conditions, and even only in the presence of low concentrations of Mg^{2+}, the chromatin fragments appear as compact circular structures (Fig. 2a, c, d). The observed height (~14 nm for fragments containing 13–18 nucleosomes; see Table 2) is similar to that obtained in previous detailed TEM measurements performed with unidirectional-shadowed preparations (~15 nm height for fibers containing 15 nucleosomes in the presence of low Mg^{2+} concentrations; see Fig. 2 in Bartolomé et al. 1994). Unfortunately, the lateral distortion of the images produced by the relatively large dimensions of the tip used for imaging is very high; the apparent diameter of the observed structures is ~82 nm (Table 2). Considering a tip radius of ~20 nm, we estimate that the actual diameter is roughly 40 nm; this value is consistent with the diameter obtained by TEM (~35 nm). Finally, as observed by TEM, we have seen extended fibers only at very low buffer concentrations (Fig. 2b).

In order to investigate the folding directly in solution using other procedures, we have centrifuged CE chromatin fragments on sucrose gradients with and without Mg^{2+}. The presence of 0.5 mM Mg^{2+} increases significantly the sedimentation velocity (Fig. 3a), suggesting that even a low concentration of this cation produces a significant chromatin folding. TEM micrographs of samples from these gradients confirm this interpretation. Individual nucleosomes can be seen in the sample sedimented in gradients without Mg^{2+} (Fig. 3b); the sample sedimented in the presence of Mg^{2+} forms the typical chromatin compact structures of ~35 nm (Fig. 3c).

Finally, we have used trypsin as a structural probe. In low ionic strength solutions without Mg^{2+}, histones H1–H5 from CE chromatin fragments can be completely digested with trypsin before any appreciable digestion of core histones (H2A, H2B, H3, and H4) occurs (Fig. 4d). In contrast, digestion in 1.7 mM Mg^{2+} (Fig. 4b, c) produces a significant degradation of H1–H5 and core histones simultaneously. This suggests that in this buffer

Table 1 Structural states of CE chromatin fragments as a function of ionic conditions

Observed structures[a]	Buffer	Cation concentrations (mM)		
		Na^+	K^+	Mg^{2+}
Nucleosomes visible	0.5–10 mM TEA			
Compact circular structures	10 mM TEA			0.5–1.7
		20	120	0–1.7
	10 mM phosphate	20	120	0–1.7
Higher aggregates	10 mM TEA			1.7–20
		20	120	1.7–20
	10 mM phosphate	20	120	1.7–20

[a]The conditions shown correspond to the regions in which the indicated structures are more frequently observed; coexistence of structures was observed in the boundaries between regions

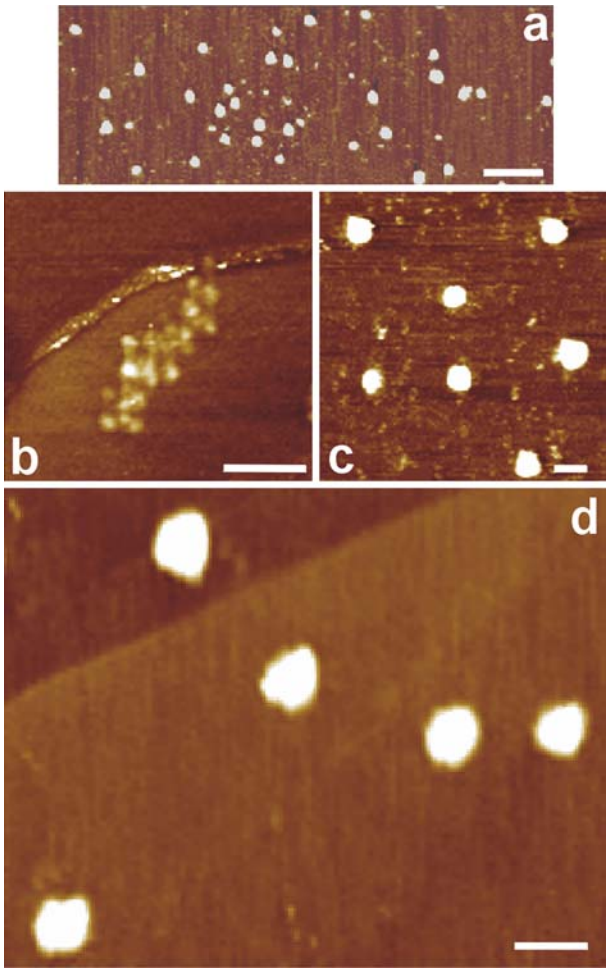

Fig. 2 **a** AFM image of folded CE chromatin fragments in the presence of solutions containing 10 mM TEA and 0.8 mM $MgCl_2$. Higher magnification AFM images of chromatin fragments in 10 mM TEA buffer containing 0.8 mM $MgCl_2$ (**c**) and 20 mM NaCl, 120 mM KCl and 1.7 mM $MgCl_2$ (**d**); **b** extended fibers in 1 mM TEA without cations. **a**, **c** Chromatin fragments containing ~18 nucleosomes were deposited on mica; **b**, **d** fragments containing ~13 nucleosomes were deposited on graphite. *Bars*: 500 nm (**a**); 100 nm (**b**–**d**)

the folding is more compact and protects almost equally H1–H5 and core histones against trypsin digestion. The electron micrographs in Fig. 4e, f show that a slight digestion in the presence of Mg^{2+} increases significantly the size of the compact chromatin bodies, indicating that they are partially unfolded. A higher degree of digestion produces unfolded structures in which individual nucleosomes and small aggregates containing few nucleosomes are visible (Fig. 4g); digestion of linker histones produces equivalent structures (Fig. 4h). A more complete denaturation, allowing the visualization of DNA (Fig. 4i), requires the use of high salt concentrations for the dissociation of histones.

These observations, and the AFM and sedimentation results, demonstrate that the size and physical behavior of chromatin fragments in solution can be perfectly correlated with the dimensions and structural properties of chromatin observed by TEM. The high folding efficiency of Mg^{2+} observed in all these experiments, has also been observed in solution studies performed with isolated individual mitotic chromosomes (Poirier et al. 2002), and could be related with the high amount of Mg^{2+} that is found homogeneously distributed in condensed chromatids during mitosis (Strick et al. 2001). The concentration of Mg^{2+} bound to isolated metaphase chromosomes (12–22 mM) is significantly higher than the average concentration found for this cation in bulk chromatin during mitosis (5–17 mM; see Introduction). This indicates that the fraction of Mg^{2+} bound to chromosomes is high, and suggests that throughout the cell cycle a significant part of the total amount of cations is not free due to the association with chromatin which is present at a high concentration in the cell nucleus.

Our results show that chromatin in solution is highly folded even under relatively low cation concentrations. The resolution attainable with AFM in aqueous solutions is not high enough to suggest a detailed structural model for chromatin folding. However, from our previous structural studies based on TEM results, we have modeled the compact circular structures as interdigitated solenoids with a local DNA concentration of about 0.27 g/ml (Daban 2003). This value is similar to that found by Leforestier et al. (1999) for dense columnar hexagonal liquid crystalline phases formed by aggregation of nucleosome core particles (0.25 g of DNA/ml), but is much higher than the local DNA concentration corresponding to irregular zigzag models (Leuba et al. 1994; Bednar et al. 1998) and more than twofold higher than the DNA concentration in the typical solenoid

Table 2 AFM measurements of CE chromatin fragments on different substrates in presence of aqueous solutions containing 10 mM TEA and different cation concentrations

Cation concentrations (mM)			Substrate	Glutaraldehyde (%)	Height[a] (nm)	Apparent diameter[a] (nm)	Number of nucleosomes per fragment	Number of particles measured
Na^+	K^+	Mg^{2+}						
		0.8	Mica	0.01	14.1 ± 2.9	81.6 ± 5.7	~18	34
20	120	1.7	Mica	0.02	12.2 ± 3.1	80.7 ± 6.9	~13	36
			Graphite	0.04	15.9 ± 2.7	82.6 ± 7.2	~13	76

[a]For each particle we have obtained the mean of two orthogonal measurements (top-bottom and left–right, with respect to the AFM field). The values shown in the table for each condition correspond to the mean of all measurements ± one standard deviation

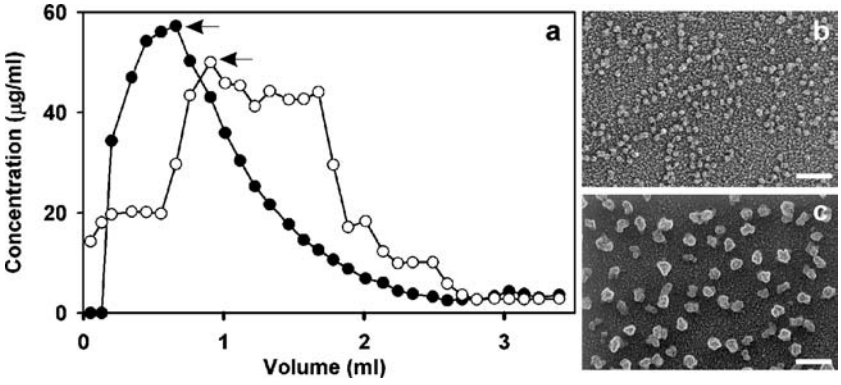

Fig. 3 Folding of chromatin fragments in solution. **a** Sedimentation profile obtained with sucrose gradients containing 10 mM TEA (*filled circle*) and the same buffer plus 0.5 mM $MgCl_2$ (*open circle*). The fractions with the highest DNA concentration (indicated with *arrows*) were analyzed by TEM: gradient with (**c**) and without (**b**) Mg^{2+}. *Bars*: 100 nm

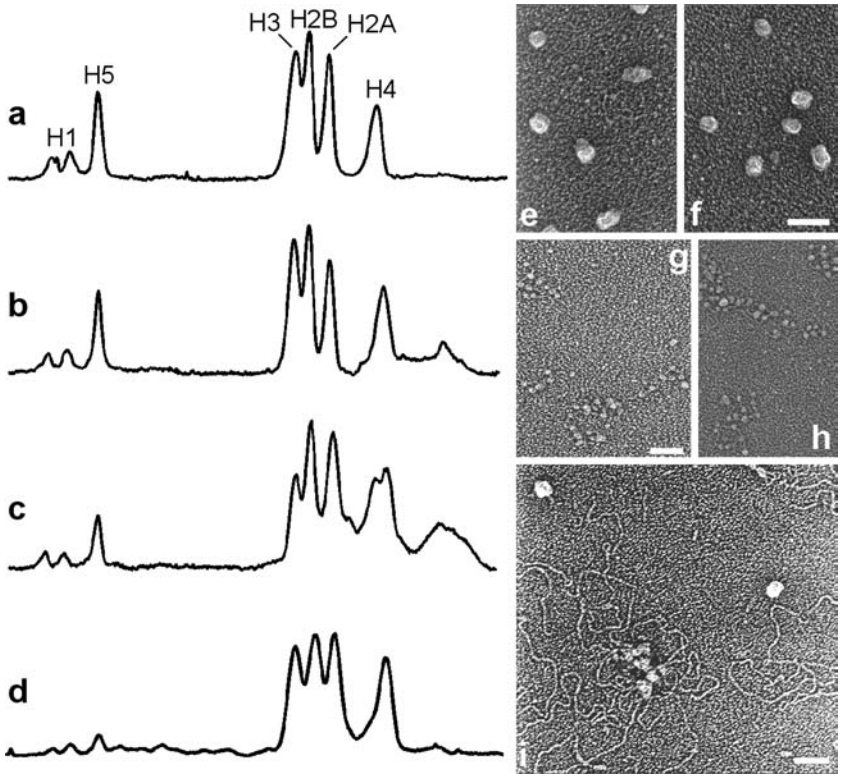

Fig. 4 Scans of SDS-polyacrylamide gels of histones from chromatin fragments digested with trypsin in the absence (**d**) and in presence (**b**, **c**) of Mg^{2+} (1.7 mM); undigested sample (**a**). The samples in **b** and **c** were digested with 0.03 and 0.3 μg/ml of trypsin, respectively; the broad band (faster than H4) in these scans contains fragments produced by core histone digestion. **e**, **f** Chromatin digested as in **b**; **g** chromatin digested as in **c**; **h** chromatin digested as in **d**. **i** Fragments crosslinked with 0.1% glutaraldehyde (30 min at 0°C) in 1.7 mM $MgCl_2$ and then treated with 0.8 M NaCl. The *bars* in micrographs **e** and **f**, **g** and **h**, and **i**, represent 100 nm

(Widom and Klug 1985). The dense folding observed in this study for chromatin in solution is important from a biological point of view, because it has been shown (Daban 2000) that with low-density chromatin fibers it is not possible to build chromatids having the high local concentration of DNA found in metaphase chromosomes.

On the other hand, note that the high compaction of chromatin in solution under interphase ionic conditions observed in this study poses more difficult structural problems for gene expression than those generally considered in current chromatin literature, which generally assumes a much less compact structure for interphase chromatin. The dramatic unfolding that presumably occurs in active genes could be produced in vivo by dynamic mechanisms such as those involving transient H1 dissociation (Misteli et al. 2000; Lever et al. 2000) and multiple covalent modifications of histones (Strahl and Allis 2000; Schübeler et al. 2004).

Acknowledgements Work supported by grants BMC2002–3948 and BFU2005-3883 (MEC-FEDER) and 2001SGR199 (Generalitat). S.C. and J.M.C. were supported by predoctoral fellowships from MEC, and M.M. by a predoctoral fellowship from the Generalitat. Cell culture was performed in the Servei de Cultius Cel·lulars (IBB). TEM and AFM images were obtained in the Servei de Microscòpia (UAB) and in the Serveis Científicotècnics (UB). The analysis of electrophoretic gels and the scanning of micrographs were performed in the Laboratori d'Anàlisi i Fotodocumentació.

References

Alberts B, Johnson A, Lewis J, Raff M, Roberts K, Walter P (2002) Molecular biology of the cell, 4th edn. Garland Science, New York

Aragay AM, Fernandez-Busquets X, Daban JR (1991) Different mechanisms for in vitro formation of nucleosome core particles. Biochemistry 30:5022–5032

Arents G, Burlingame RW, Wang BC, Love WE, Moudrianakis EN (1991) The nucleosomal core histone octamer at 3.1 Å resolution: a tripartite protein assembly and a left-handed superhelix. Proc Natl Acad Sci USA 88:10148–10152

Bartolomé S, Bermúdez A, Daban JR (1994) Internal structure of the 30 nm chromatin fiber. J Cell Sci 107:2983–2992

Bartolomé S, Bermúdez A, Daban JR (1995) Electrophoresis of chromatin on nondenaturing agarose gels containing Mg^{2+}. Self-assembly of small chromatin fragments and folding of the 30-nm fiber. J Biol Chem 270:22514–22521

Bednar J, Horowitz RA, Grigoryev SA, Carruthers LM, Hansen JC, Koster AJ, Woodcock CL (1998) Nucleosomes, linker DNA, and linker histone form a unique structural motif that directs the higher-order folding and compaction of chromatin. Proc Natl Acad Sci USA 95:14173–14178

Bordas J, Perez-Grau L, Koch MHJ, Vega MC, Nave C (1986) The superstructure of chromatin and its condensation mechanism: II Theoretical analysis of the X-ray scattering patterns and model calculations. Eur Biophys J 13:175–185

Bustamante C, Zuccheri G, Leuba SH, Yang G, Samori B (1997) Visualization and analysis of chromatin by scanning force microscopy. Methods 12:73–83

Caravaca JM, Caño S, Gállego I, Daban JR (2005) Structural elements of bulk chromatin within metaphase chromosomes. Chromosome Res 13:725–743

Daban JR (2000) Physical constraints in the condensation of eukaryotic chromosomes. Local concentration of DNA versus linear packing ratio in higher order chromatin structures. Biochemistry 39:3861–3866

Daban JR (2003) High concentration of DNA in condensed chromatin. Biochem Cell Biol 81:91–99

Daban JR, Bermúdez A (1998) Interdigitated solenoid model for compact chromatin fibers. Biochemistry 37:4299–4304

Davies E, Teng KS, Conlan RS, Wilks SP (2005) Ultra-high resolution imaging of DNA and nucleosomes using non-contact atomic force microscopy. FEBS Lett 579:1702–1706

Grigoryev SA (2004) Keeping fingers crossed: heterochromatin spreading through interdigitation of nucleosome arrays. FEBS Lett 564:4–8

Hansen JC (2002) Conformational dynamics of the chromatin fiber in solution: determinants, mechanisms, and functions. Annu Rev Biophys Biomol Struct 31:361–392

Harp JM, Hanson BL, Timm DE, Bunick GJ (2000) Asymmetries in the nucleosome core particle at 2.5 Å resolution. Acta Crystallogr D 56:1513–1534

Leforestier A, Fudaley S, Livolant F (1999) Spermidine-induced aggregation of nucleosome core particles: evidence for multiple liquid crystalline phases. J Mol Biol 290:481–494

Leuba SH, Yang G, Robert C, Samori B, van Holde K, Zlatanova J, Bustamante C (1994) Three-dimensional structure of extended chromatin fibers as revealed by tapping-mode scanning force microscopy. Proc Natl Acad Sci USA 91:11621–11625

Leuba SH, Zlatanova J, Karymov MA, Bash R, Liu YZ, Lohr D, Harrington RE, Lindsay SM (2000) The mechanical properties of single chromatin fibers under tension. Single Mol 1:185–192

Lever MA, Th'ng JPH, Sun X, Hendzel MJ (2000) Rapid exchange of histone H1.1 on chromatin in living human cells. Nature 408:873–876

Levi-Setti R (1988) Structural and microanalytical imaging of biological materials by scanning microscopy with heavy-ion probes. Annu Rev Biophys Biophys Chem 17:325–347

Luger K, Mäder AW, Richmond RK, Sargent DF, Richmond TJ (1997) Crystal structure of the nucleosome core particle at 2.8 Å resolution. Nature 389:251–260

Marko JF, Poirier MG (2003) Micromechanics of chromatin and chromosomes. Biochem Cell Biol 81:209–220

Misteli T, Gunjan A, Hock R, Bustin M, Brown DT (2000) Dynamic binding of histone H1 to chromatin in living cells. Nature 408:877–881

Mozziconacci J, Victor JM (2003) Nucleosome gaping supports a functional structure for the 30 nm chromatin fiber. J Struct Biol 143:72–76

Poirier MG, Monhait T, Marko JF (2002) Reversible hypercondensation and decondensation of mitotic chromosomes studied using combined chemical-micromechanical techniques. J Cell Biochem 85:422–434

Richmond TJ, Davey CA (2003) The structure of DNA in the nucleosome core. Nature 423:145–150

Rill RL, Shaw BR, van Holde KE (1978) Isolation and characterization of chromatin subunits. Methods Cell Biol 18:69–103

Schalch T, Duda S, Sargent DF, Richmond TJ (2005) X-ray structure of a tetranucleosome and its implications for the chromatin fibre. Nature 436:138–141

Schübeler D, MacAlpine DM, Scalzo D, Wirbelauer C, Kooperberg C, van Leeuwen F, Gottschling DE, O'Neill LP, Turner BM, Delrow J, Bell SP, Groudine M (2004) The histone modification pattern of active genes revealed through genome-wide chromatin analysis of a higher eukaryote. Genes Dev 18:1263–1271

Strahl BD, Allis CD (2000) The language of covalent histone modifications. Nature 403:41–45

Strick R, Strissel PL, Gavrilov K, Levi-Setti R (2001) Cation-chromatin binding as shown by ion microscopy is essential for the structural integrity of chromosomes. J Cell Biol 155:899–910

Subirana JA, Muñoz-Guerra S, Aymamí J, Radermacher M, Frank J (1985) The layered organization of nucleosomes in 30 nm chromatin fibers. Chromosoma 91:377–390

Sumner AT (2003) Chromosomes: organization and function. Blackwell Publishing, Oxford

White CL, Suto RK, Luger K (2001) Structure of the yeast nucleosome core particle reveals fundamental changes in internucleosome interactions. EMBO J 20:5207–5218

Widom J (1986) Physicochemical studies of the folding of the 100 Å nucleosome filament into the 300 Å filament. Cation dependence. J Mol Biol 190:411–424

Widom J (1998) Structure, dynamics and function of chromatin in vitro. Annu Rev Biophys Biomol Struct 27:285–327

Widom J, Klug A (1985) Structure of the 300 Å chromatin filament: X-ray diffraction from oriented samples. Cell 43:207–213

Williams SP, Langmore JP (1991) Small angle X-ray scattering of chromatin. Radius and mass per unit length depend on linker length. Biophys J 59:606–618

Williams SP, Athey BD, Muglia LJ, Schappe RS, Gough AH, Langmore JP (1986) Chromatin fibers are left-handed double helices with diameter and mass per unit length that depend on linker length. Biophys J 49:233–248

Wolffe AP (1998) Chromatin structure and function, 3rd edn. Academic, London

Woodcock CL, Dimitrov S (2001) Higher-order structure of chromatin and chromosomes. Curr Opin Genet Dev 11:130–135

Woodcock CL, Horowitz RA (1997) Electron microscopy of chromatin. Methods 12:84–95

Zentgraf H, Franke WW (1984) Differences of supranucleosomal organization in different kinds of chromatin: cell type-specific globular subunit containing different numbers of nucleosomes. J Cell Biol 99:272–286

Zlatanova J, Leuba SH (2003) Chromatin fibers, one-at-a-time. J Mol Biol 331:1–19